LITHOS 426–427 (2022) 106795

Contents lists available at ScienceDirect

LITHOS

journal homepage: www.elsevier.com/locate/lithos

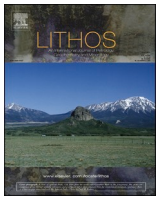

Mantle plume–stagnant slab interaction controls the generation of a mixed mantle source for continental intraplate basalts

Xun Yu [a,*], Zhifei Liu [a], Gang Zeng [b], Wenrong Cao [c], Rithy Meas [d], Long Van Hoang [e], Pham Nhu Sang [a]

[a] State Key Laboratory of Marine Geology, Tongji University, Shanghai 200092, China
[b] State Key Laboratory for Mineral Deposits Research, School of Earth Sciences and Engineering, Nanjing University, Nanjing 210023, China
[c] Department of Geological Sciences and Engineering, University of Nevada, Reno 89557, USA
[d] Department of Marine and Coastal Zone Conservation, Ministry of Environment, Phnom Penh, Cambodia
[e] Vietnam Petroleum Institute, Hanoi, Viet Nam

ARTICLE INFO

Keywords:
Continental intraplate basalt
Mantle plume
Basalt geochemistry
Stagnant slab
Cambodia
South China Sea

ABSTRACT

Continental intraplate basalts from southeastern Eurasia show ocean island basalt-like geochemical signatures and heterogeneous isotopic compositions suggesting mixing between isotopically enriched and depleted end-member sources. Although the isotopically enriched end-member(s) in these basalts which are related to oceanic crustal recycling have been investigated, the nature of the isotopically depleted end-member(s) remains unclear. We present geochemical characteristics of the southeast Cambodia basalt and compare them with other Cenozoic intraplate basalts in the South China Sea region. All these basalts contain a component with low Ce/Pb and Nb/Th ratios, moderate $^{87}Sr/^{86}Sr$ (~0.7040) and ε_{Nd} (~ + 5), high ε_{Hf} (~ + 9.5), and slightly positive $\Delta\varepsilon_{Hf}$ value. These chemical and isotopic signatures are not consistent with the depleted local asthenosphere. We suggest a FOZO-like component, which is most likely derived from lower mantle material, represents the low-Ce/Pb component. Combined with geophysical observations, we propose that the interaction between the upwelling mantle plume and the stagnant slabs controls the formation of these intraplate basalts from the South China Sea region. This study highlights the important role of stagnant slabs in the mantle transition zone in modifying the compositions of mantle plumes, ultimately resulting in upper mantle heterogeneity.

1. Introduction

Mantle plumes link the deep mantle to the Earth's surface and have commonly been studied in rift and intraplate settings, where stagnant subducted oceanic slabs in the mantle transition zone (410–660 km) are absent (e.g., Condie, 2001; Kincaid et al., 1995; White et al., 1993). However, the behavior of mantle plumes near subduction zones remains poorly understood (e.g., Kincaid et al., 2013; Mériaux et al., 2016). Numerical calculations show that a peridotitic diapir from the lower mantle can entrain fragments of oceanic crust that have stagnated at the mantle transition zone, thereby forming a mixed plume of upwelling material (Yasuda and Fujii, 1998). Such a model is supported by geophysical evidence from the modern Cascadia subduction zone and Yellowstone hotspot in the western North America, and the interaction between the Tonga–Kermadec oceanic slab and the Samoan mantle plume in the Southwest Pacific (Chang et al., 2016; Leonard and Liu, 2016). However, geological observations from each of these regions are not entirely consistent with the conventional view of mantle plumes. For example, the spatial age progression of volcanic rocks in the Yellowstone region cannot be explained by a single plume model (Christiansen et al., 2002; Leonard and Liu, 2016). This may be due to the behavior of the upwelling plume being affected by the stagnant slab (Kincaid et al., 2013). Approximately 50% of recognized mantle plumes dating back to 60 Ma lie within 1000 km of subduction zones (Fletcher and Wyman, 2015). Hence, the role of mantle plume–stagnant slab interactions on the upwelling plume and development of upper mantle heterogeneity needs to be further investigated.

Cenozoic intraplate basalts are widely developed in the South China Sea region, which is surrounded by multiple subduction systems (Barr and Macdonald, 1981; Ho et al., 2003; Li et al., 2014; Xu et al., 2012) (Fig. 1a). Notably, all these basalts show ocean island basalt (OIB)-like geochemical features and record the mixing between relatively depleted

* Corresponding author.
E-mail address: yuxun@tongji.edu.cn (X. Yu).

https://doi.org/10.1016/j.lithos.2022.106795
Received 22 February 2022; Received in revised form 30 June 2022; Accepted 30 June 2022
Available online 7 July 2022

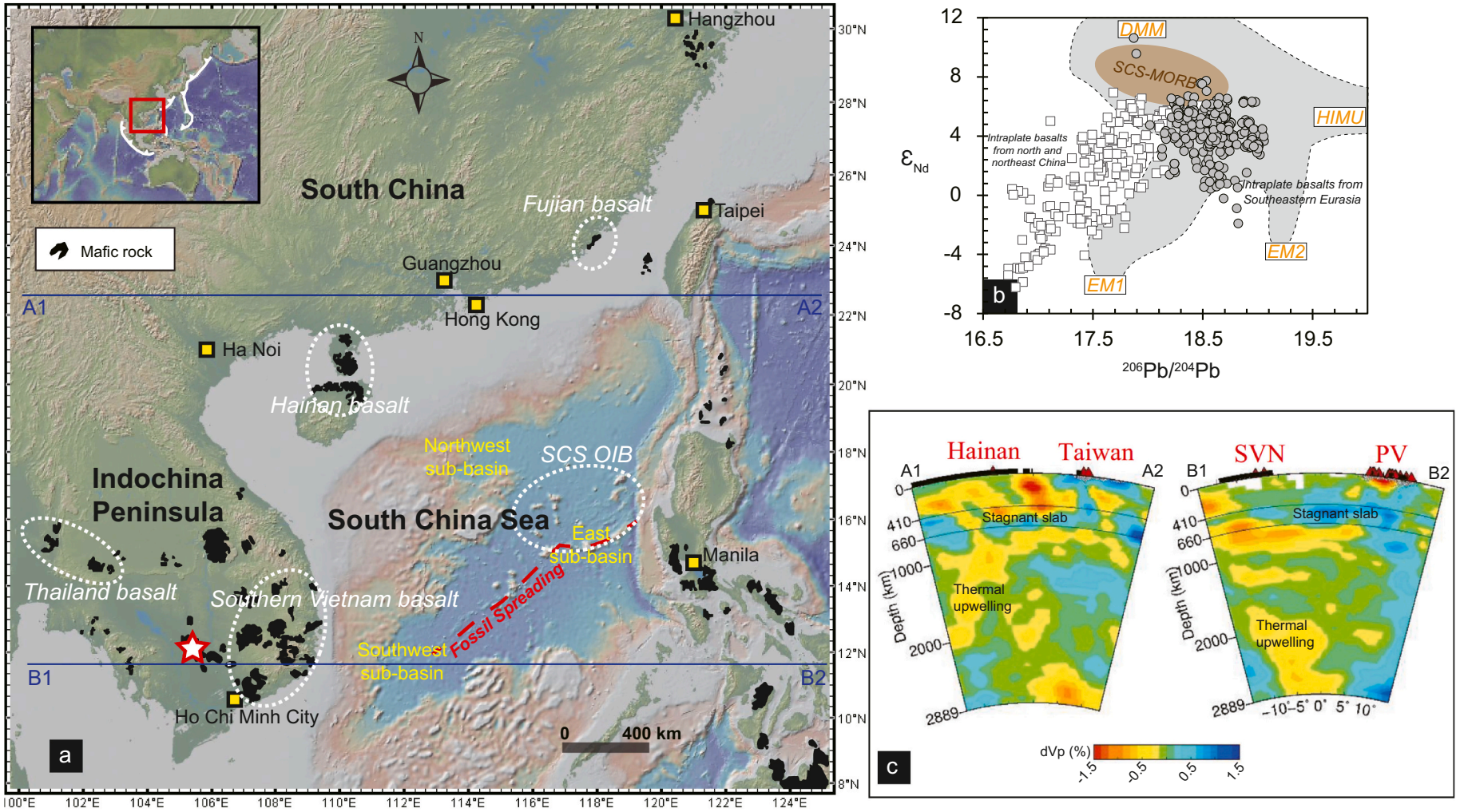

Fig. 1. Topographic map of southeast Asia and distribution of Cenozoic mafic volcanisms (a), Pb and Nd isotopic compositions of Cenozoic basalts from eastern Eurasia (b), and vertical cross-sections of P-wave tomography (c). Figure (a) is made with GeoMapApp 3.6.6 (www.geomapapp.org) and distribution of Cenozoic mafic volcanisms is modified from Xu et al. (2012). Basalt data in figure (b) is derived from GEOROC database. In figure (c), Vertical cross-sections of P-wave tomography from the Earth's surface down to the core-mantle boundary along the profiles in (a) are after Zhao et al. (2021). The red and blue colors denote low and high velocity perturbations, respectively, as shown by the colour bar with numbers below. The red triangles atop each cross-section denote the locations of active volcanoes. The two dashed black lines denote the 410 and 660 km discontinuities of the mantle transition zone. The flat high-velocity anomaly in the mantle transition zone was interpreted as representing the stagnant slabs (e.g., Zhao et al. (2021)), and the subvertical low-velocity anomaly crossing the mantle transition zone into the upper and lower mantle was interpreted as the thermal upwellings (e.g., Zhao et al. (2021)). SVN, volcanoes in southern Vietnam; PV, volcanoes in Philippines. (For interpretation of the references to colour in this figure legend, the reader is referred to the web version of this article.)

and EM2-type enriched mantle components (Zou et al., 2000) (Fig. 1b). Recycled oceanic crustal materials are mostly thought to be responsible for the EM2-type enriched mantle component in the South China Sea region (e.g., An et al., 2017; Hoang et al., 2018; Yu et al., 2019; Zeng et al., 2017). Mantle potential temperatures estimated from these basalts reveal the thermal anomaly, suggesting the occurrence of the Hainan mantle plume beneath the region (An et al., 2017; Wang et al., 2012; Yan and Shi, 2008; Yang et al., 2019). This is supported by geophysical observations of continuous low-velocity bodies that extend into the lower mantle near Hainan Island (Huang and Zhao, 2006; Xia et al., 2016) (Fig. 1c). In addition, seismic observations have shown that a large number of stagnant slabs are present in the mantle transition zone, likely demonstrating the occurrence of mantle plume–subduction zone interactions in this region (Mériaux et al., 2015; Zhao et al., 2021). However, there is no geological evidence for such a mantle plume model. Large-scale and long-lived magmatism has not occurred in the South China Sea region (Sun, 2016), and there is no direct geochemical evidence (i.e., high $^{3}He/^{4}He$ ratios) supporting the direct contribution from a mantle plume (e.g., Qian et al., 2021). Therefore, due to subduction of the Indian–Australian and Pacific plates, the intraplate basalts formed in the South China Sea region are ideal materials for investigating the interaction between mantle plumes and subduction systems and generating upper mantle heterogeneity.

Here we report new whole-rock major and trace elemental compositions and Sr–Nd–Hf isotope data for southeast Cambodia basalts which are located to the west of the southern Vietnam basaltic fields (Fig. 1a). These data are the first for intraplate basalts from the central Indochina Peninsula, where diffuse igneous provinces dominate (Hoang and Flower, 1998). We compare our data with those for other basalts from the South China Sea region. Our data and geophysical observations together provide new insights into the relationship between continental intraplate basalt, oceanic subduction, and seismically detected mantle plume.

2. Geologic background and sampling

The tectonic evolution of the South China Sea region (i.e., South China Sea basin, Indochina Block, and South China Block) has been influenced by the northwestward subduction of the Paleo-Pacific Plate, northeastward subduction of the Indian–Australian Plate, and collision between the Indian–Australian and Eurasian plates since the mid- to late Mesozoic (Hall (2002), Fig. 1a). After termination of seafloor spreading in the South China Sea basin (spreading occurred during 34–15 Ma), numerous, small-scale, and genetically related intraplate basaltic fields have formed within and around the South China Sea basin (Ho et al., 2003; Xu et al., 2012). These intraplate volcanic fields can be divided into six areas from northeast to southwest: Fujian basalts (<19 Ma), Hainan basalts (<17 Ma), South China Sea OIBs (<19 Ma), southern Vietnam basalts (<17 Ma), Cambodia basalts (<15 Ma), and Thailand basalts (<24 Ma) (Barr and Macdonald, 1981; Ho et al., 2003; Hoang et al., 2018; Yan et al., 2018). The eruptive units in southern Vietnam and eastern Cambodia are the most voluminous in the Indochina Peninsula and crop out over an area of ~70,000 km^2 (Hoang et al., 2018, and reference therein) (Fig. 1a).

In Cambodia, basaltic rocks are mainly distributed in the eastern part of the country. The northern side of the basaltic field spatially continues with the Pleiku basaltic field of southern Vietnam that erupted at ~6 Ma, while the south side of the basaltic field can be regarded as the westward extension of the Phuoc Long basaltic field of southern Vietnam that erupted at ~15 Ma (An et al., 2017; Barr and Macdonald, 1981; Hoang and Flower, 1998). Sixteen basalt samples were collected in this study from the north to east of Kampong Cham city in southeastern Cambodia (Fig. S1; Table S1), and we term the southeast Cambodia basalts. In hand specimen, all basalts exhibit black to dark grey in colour, massive to vesicular structure (Fig. S2a). Most samples are fresh, and only a few are slightly altered with minor olivine being partially decomposed to iddingsite. These samples are either porphyritic (Fig. S2b) or aphyric (Fig. S2c) in texture. Basalts with porphyritic texture contain minor olivine phenocrysts (<10% modal abundance) set in a groundmass composed of plagioclase, olivine, clinopyroxene, Fe—Ti oxides, and glass. The diameter of olivine grain is <1 mm. No crustal and mantle xenoliths are found in these basalts.

For geochemical comparison, crustal xenoliths hosted by late Cenozoic basalts were collected from southern Vietnam (near Dalat city) to the east of Cambodia. The Dalat basaltic flows consist of four major phases (16.7–6.3 Ma, 4.0–2.1 Ma, 1.8–0.9 Ma, and 0.7–0.4 Ma), crop out over an area of ~3500 km^2, and are up to 300 m thick (Hoang et al., 1996; Hoang et al., 2018). Four crustal xenoliths reported in this study contain three mafic crustal xenoliths and one felsic crustal xenolith. The mafic crustal xenoliths are two-pyroxene granulites that consist of clinopyroxene, orthopyroxene, plagioclase, and opaque accessory minerals with granoblastic microstructures (Fig. S2d). The felsic crustal xenolith is composed of quartz, plagioclase, and orthopyroxene with granoblastic microstructure. These crustal xenoliths are fresh and show similar petrographical features to lower crustal xenoliths from southeast China (Yu et al., 2003).

3. Results

Major and trace elemental compositions as well as Sr, Nd, and, Hf isotopic compositions are measured for Cambodia basalt samples, while Sr, Nd, and Hf isotopic compositions are only analyzed for the lower crustal xenoliths. A detailed description of analytical methods is present in the Appendix. New elemental and isotopic data for southeast Cambodia basalts are listed in Table S2, and those for international standards and reduplicated samples during basaltic sample analyses are also given in Table S2. New isotopic data for lower crustal xenoliths are listed in Table S3.

The southeast Cambodia samples are basalts and trachybasalts (Fig. 2a), which have homogeneous SiO_2 (47.7–49.4 wt%), variable MgO (6.01–11.1 wt%), high FeO^T (10.2–11.7 wt%), and moderate TiO_2 (1.81–2.24 wt%) contents (Fig. 2a–d). In the plot of CaO/Al_2O_3 versus MgO, a positive correlation is seen for samples with MgO > 9 wt% and a weakly negative correlation is shown for samples with MgO < 9 wt% (Fig. 2b). The similar geochemical pattern is observed from the plot of FeO^T versus MgO, wherein flat trend is seen for samples with MgO > 9 wt% and a positive correlation is seen for samples with MgO < 9 wt% (Fig. 2c). The southeast Cambodia basalts contain 66.0–295 ppm Ni, and 18.1–21.5 ppm Sc, wherein MgO is positively correlated with Ni (Fig. 2e) but showing no correlation with Sc (Fig. 2f). These samples exhibit enrichments in highly incompatible elements, positive Nb and Ta anomalies, and negative Pb, Zr, and Hf anomalies (Fig. 3a), similar to typical OIBs (Niu and O'Hara, 2003). The samples do not have Eu anomalies (Fig. 3b).

For the southeast Cambodia basalts, ε_{Nd} values correlate negatively with $^{87}Sr/^{86}Sr$ (Fig. 4a), and there is a weak negative correlation between ε_{Nd} and ε_{Hf} values (Fig. 4b). $^{87}Sr/^{86}Sr$ ratios correlate negatively with Ce/Pb ratios, and ε_{Nd} values correlate positively with Ce/Pb ratios (Fig. 4c–d). For the lower crustal xenoliths, we can divide them into two groups according to their whole-rock Sr, Nd, and Hf isotopic compositions (Fig. 4a–b) as high-ε_{Nd} group ($^{87}Sr/^{86}Sr$ = 0.703578 to 0.703688, ε_{Nd} = +5.1 to +5.4, ε_{Hf} = +7.0 to +7.2) and low-ε_{Nd} group ($^{87}Sr/^{86}Sr$ = 0.705105 to 0.705197, ε_{Nd} = +0.7 to +2.8, ε_{Hf} = +2.7 to +6.2). In the plot of ε_{Hf} versus ε_{Nd}, the southeast Cambodia basalts fall below the terrestrial array and are similar to the Fujian basalts, indicating slight decoupling of ε_{Hf} from ε_{Nd}, as evident from their negative $\Delta\varepsilon_{Hf}$ values. $\Delta\varepsilon_{Hf}$ is defined as $\Delta\varepsilon_{Hf} = \varepsilon_{Hf} - (1.55 \times \varepsilon_{Nd} + 1.21)$ and quantifies the deviation of ε_{Hf} from the terrestrial array (Vervoort et al., 2011). $\Delta\varepsilon_{Hf}$ values of basalts (Fig. 4b) can be used to identify the origin of mantle source heterogeneity in the upper mantle (e.g., Chauvel et al., 2008; Chen et al., 2009; Vervoort et al., 2011; Zeng et al., 2011). For example, Indian mid-ocean ridge basalts (MORBs) and pelagic sediments have

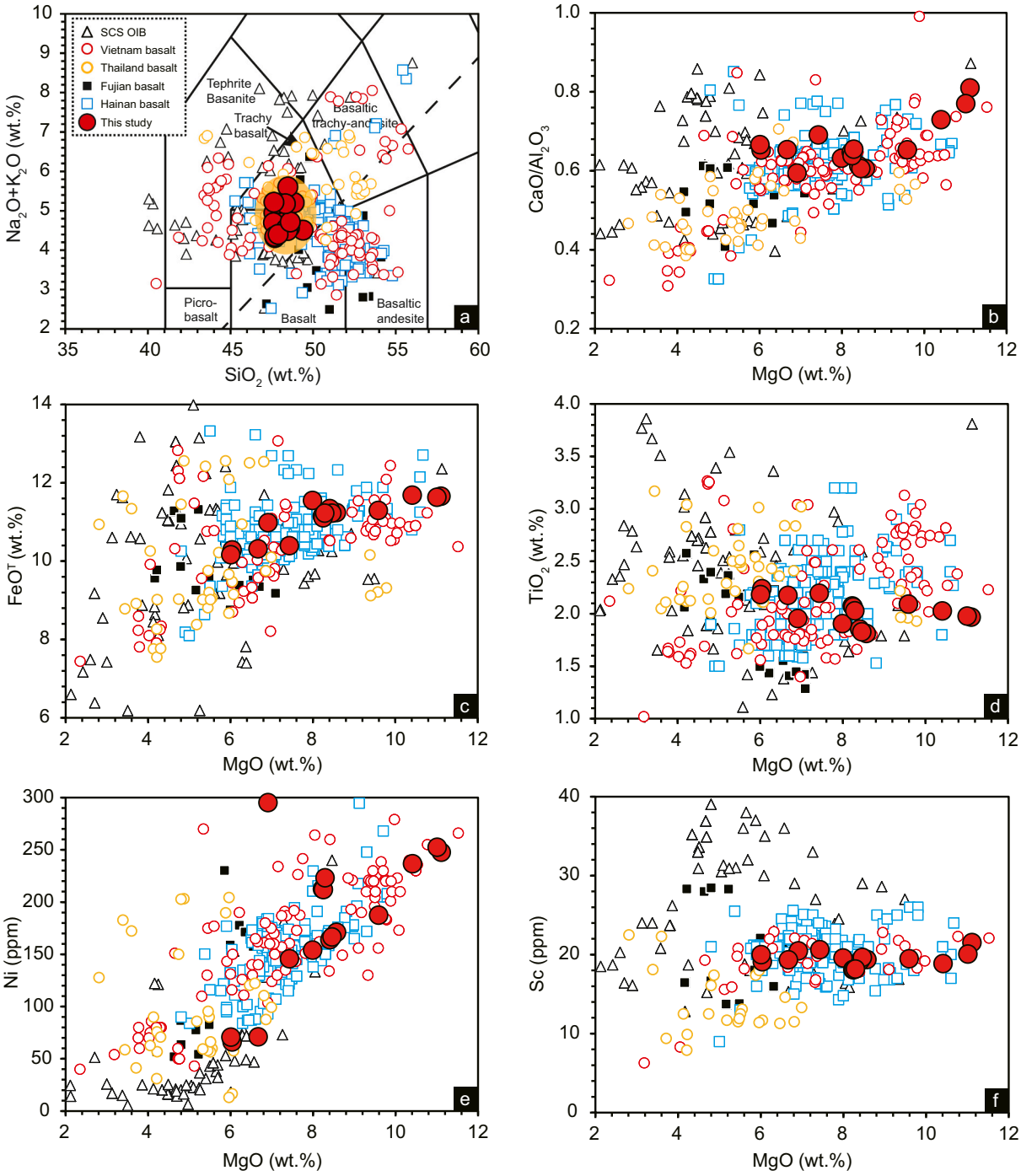

Fig. 2. Variations in SiO_2 versus $Na_2O + K_2O$ (a), MgO versus CaO/Al_2O_3 (b), FeO^T (c), TiO_2 (d), Ni (e), and Sc (f) for southeast Cambodia basalts. Classification of volcanic rocks is based on Le Bas et al. (1986). Reference data for basalt samples from the South China Sea basin (Tu et al., 1992; Yan et al., 2008; Yan et al., 2015; Zhang et al., 2017), southern Vietnam (An et al., 2017; Hoang et al., 1996; Hoang et al., 2018; Hoàng et al., 2013; Hoang and Flower, 1998), Thailand (Yan et al., 2018; Zhou and Mukasa, 1997), Fujian (Zeng et al., 2017), and Hainan (Flower et al., 1992; Mei and Ren, 2019; Tu et al., 1991; Wang et al., 2012; Wang et al., 2013) are present for comparison.

positive $\Delta\varepsilon_{Hf}$ values, whereas Pacific MORBs have negative $\Delta\varepsilon_{Hf}$ values (Chauvel et al., 2008; Pearce et al., 1999, 2007). Thus, recycling of different oceanic components back into the mantle can form intraplate basalts with variable $\Delta\varepsilon_{Hf}$ values. In the plots of Ce/Pb and Nb/Th versus $\Delta\varepsilon_{Hf}$ (Fig. 5a–b), all basalts from the South China Sea region, including the southeast Cambodia basalts, share a common end-member characterized by low Ce/Pb and Nb/Th ratios with slightly positive (but close to zero) $\Delta\varepsilon_{Hf}$ values. Various trends to high Ce/Pb ratios are also exhibited by other basalts in addition to the southeast Cambodia basalts from the South China Sea region (Fig. 5).

4. Discussion

4.1. Post-magmatic alteration, crustal contamination, and low-pressure fractional crystallization

Geochemical variations of continental intraplate basalts can be produced by shallow processes such as surface weathering and magma

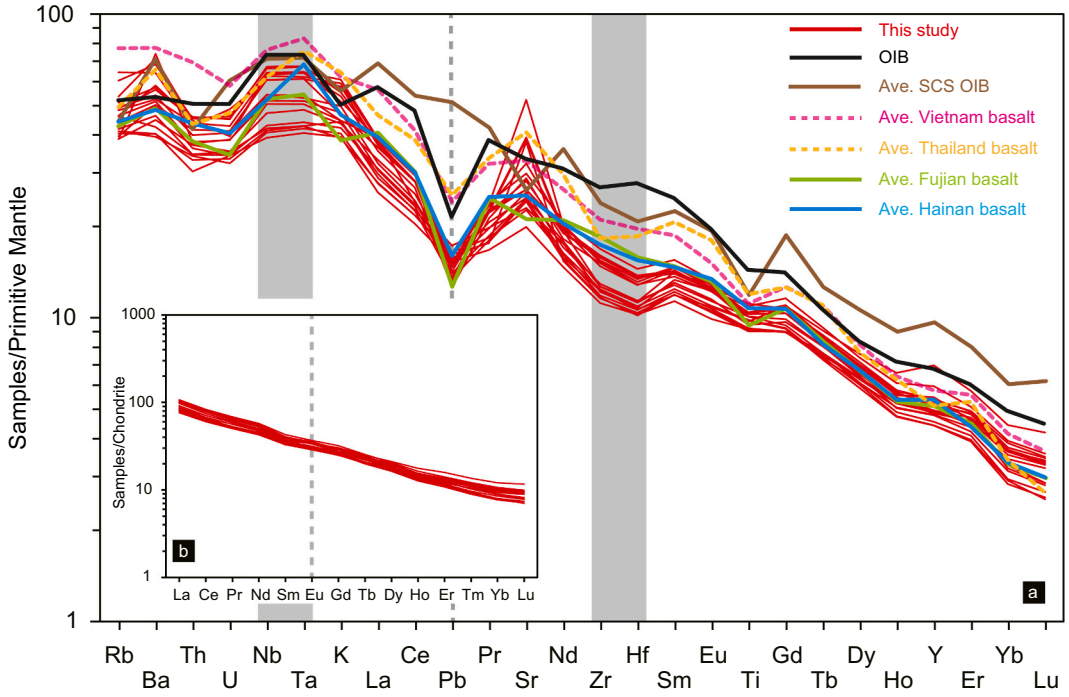

Fig. 3. Primitive-mantle-normalized incompatible element patterns (a) and Chondrite-normalized REE patterns (b) for southeast Cambodia basalts. The primitive mantle values and the chondrite values are from Anders and Grevesse (1989) and McDonough and Sun (1995), respectively. The data of representative oceanic island basalt (OIB) can be referred to Niu and O'Hara (2003). The average data for South China Sea OIB, southern Vietnam basalts, Thailand basalts, Fujian basalts, and Hainan basalts are estimated according to data from the same literature as those in Fig. 2.

chamber processes (e.g., Carlson et al., 1981; Kumar et al., 2010; Yu et al., 2015) in addition to source heterogeneity. Before we can discuss the origin of the geochemical variations of basalts, we should evaluate the influence from these shallow processes. The fresh appearance of hand specimens (Fig. S2) indicates that weathering should have little influence on the geochemical compositions. This inference can be supported by the relatively low LOI values (< 2 wt%) which have no correlations between strongly incompatible elements like La (Fig. S3a) and fluid-mobile elements like U (Fig. S3b). The minimal influence of surface weathering can also be verified by the good correlations between Nb and the strongly incompatible elements such as K, Ba, La, and U (Fig. S3c-f).

Trace element and radiogenic isotope features of the southern Vietnam basalts indicate that some samples were affected by continental crustal contamination during their petrogenesis (Hoang et al., 1996; Hoang and Flower, 1998). The upper continental crust has lower Ce/Pb and Ba/Rb ratios than the DMM (depleted MORB mantle), while the lower continental crust has lower Ce/Pb and higher Ba/Rb ratios than the DMM (Fig. 6a). The variable Ce/Pb and uniform Ba/Rb ratios of the southeast Cambodia basalts suggest there was negligible crustal contamination (Fig. 6a). Continental crust has lower MgO contents and ε_{Nd} and ε_{Hf} values than mantle-derived basalts (e.g., Rudnick and Gao, 2014), and thus crustal contamination is expected to produce a positive correlation between MgO content and Ce/Pb, ε_{Nd}, and ε_{Hf} values (e.g., An et al., 2017). However, apart from some basalt samples from southern Vietnam and Thailand, the Cambodia samples exhibit no clear correlation between MgO content and ε_{Nd} value (Fig. 6b) and exhibit a negative correlation between Ce/Pb ratio and ε_{Hf} value (Fig. 7a). We also compared the geochemical and isotopic compositions of the southeast Cambodia basalts with the lower crustal xenoliths from southern Vietnam. Although the lower crustal xenoliths show variable isotopic compositions (Fig. 4a–b), they are more enriched in isotopes than the southeast Cambodia basalts with low-Ce/Pb and low-Nb/Th ratios (Figs. 4 and 7). As such, crustal contamination is unlikely to generate the geochemical variations of southeast Cambodia basalts.

The presence of olivine phenocrysts in some Cambodia basalt samples indicates the role of olivine fractionation in some of the basaltic melts, which is suggested by the positive correlations between MgO and FeO^T and Ni contents for samples with MgO < 9 wt% (Fig. 2e). Nonetheless, no correlations are seen between MgO and FeO^T for samples with MgO > 9 wt%, excluding the role of olivine fractionation or accumulation in petrogenesis of these basalts. For basalts with MgO < 9 wt% experiencing fractional crystallization of olivine, no correlations are observed between MgO and CaO/Al_2O_3 ratios and Sc contents (Fig. 2b, f). This indicates that fractional crystallization of clinopyroxene is ignorable. For basalts with MgO > 9 wt%, the positive correlation between CaO/Al_2O_3 versus MgO could record the influence of clinopyroxene during magmatic evolution. However, no correlation is shown between TiO_2 and Sc versus MgO, excluding the effect of clinopyroxene fractionation or accumulation. The absence of a negative Eu anomaly and the lack of plagioclase phenocrysts suggest that plagioclase fractionation did not occur. At lower MgO contents, southeast Cambodia basalts show relatively constant, or slightly increased, TiO_2 contents (Fig. 2d), indicating negligible fractionation of Fe—Ti oxides and other Ti-bearing minerals. Therefore, we can conclude that fractional crystallization should not affect the geochemical variation of southeast Cambodia basalts.

4.2. *Origin of the high-Ce/Pb component: Recycled oceanic crust material*

The high-Ce/Pb end-member of southeast Cambodia basalts is characterized by a negative $\Delta\varepsilon_{Hf}$ value (< −5) with an elevated Nb/Th ratio and ε_{Nd} value but a decreased $^{87}Sr/^{86}Sr$ ratio (Figs. 4 and 5), which are similar to the intraplate basalts from the Fujian and Hainan provinces of the south China (e.g., Wang et al., 2013; Yu et al., 2019; Zeng et al., 2017). The elemental and isotopic features of such high-Ce/Pb end-member cannot be explained by the DMM or local depleted asthenosphere as represented by the South China Sea MORB which has close to zero $\Delta\varepsilon_{Hf}$ value (Fig. 7). Therefore, we infer that a recycled component similar to those enriched components in sources of the Fujian and Hainan basalts should be responsible for such a high-Ce/Pb

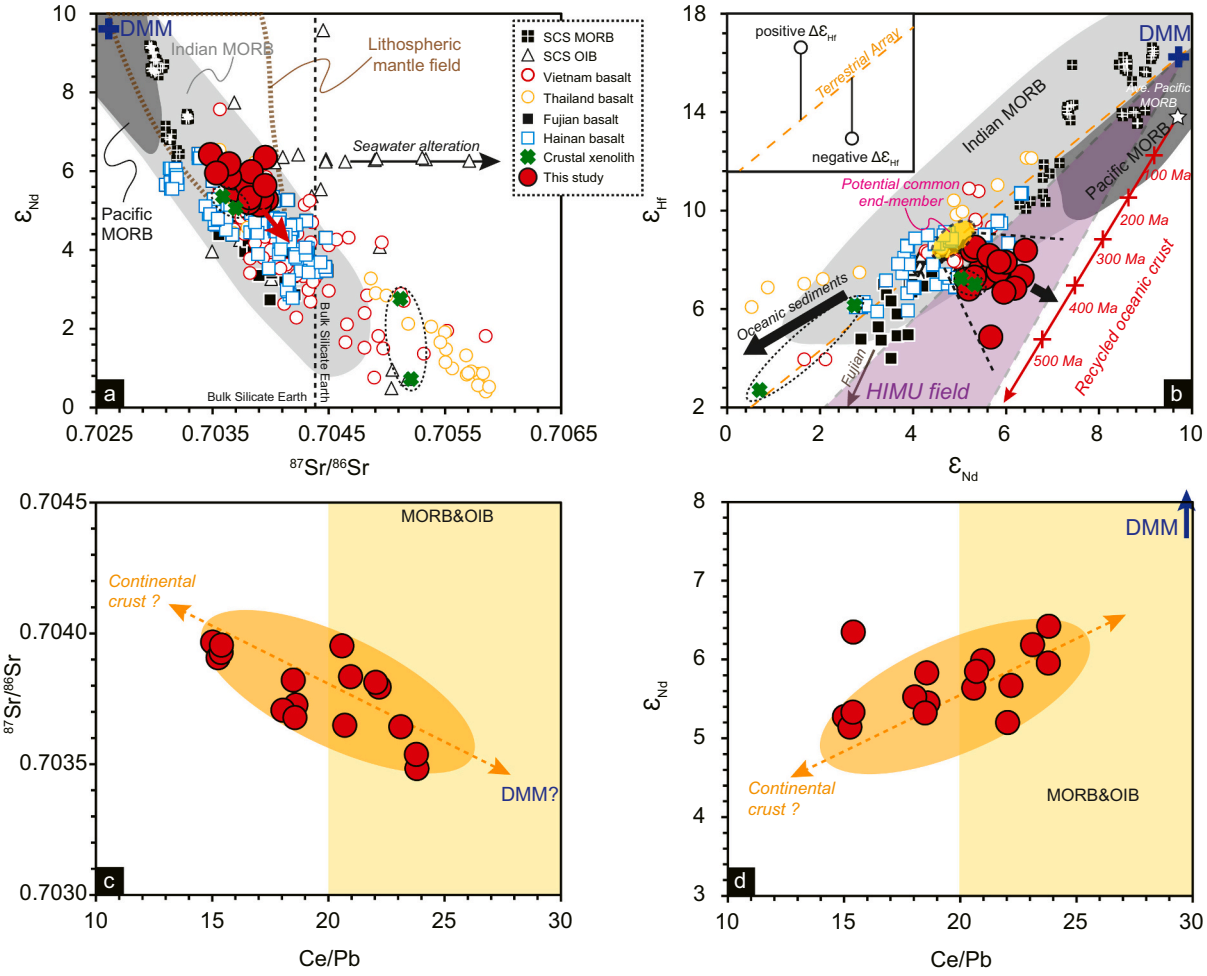

Fig. 4. Isotopic and trace elemental features of southeast Cambodia basalts. Variation in $^{87}Sr/^{86}Sr$ versus ε_{Nd} (a), ε_{Nd} versus ε_{Hf} (b), Ce/Pb versus $^{87}Sr/^{86}Sr$ (c) and ε_{Nd} (d) are present. Data for the depleted MORB mantle (DMM) are from Workman and Hart (2005). The terrestrial reference line in (b) is from Vervoort et al. (2011) and trend of oceanic sediments is from Chauvel et al. (2008). Data of global MORBs (Pacific Ocean MORB and Indian Ocean MORB) are derived from Petrological Database (http://www.earthchem.org/petdb). Data of South China Sea MORB are collected from references (Zhang et al., 2018a; Zhang et al., 2018b). The lithospheric mantle field is based on the composition of peridotite xenoliths from Cenozoic basalts of southeast China (Qi et al., 1995; Tatsumoto et al., 1992). The Nd—Hf isotopic compositions of recycled oceanic crust at various times are also shown as evolution path (red line), which was calculated by using an average, present-day isotopic composition of MORB from the East Pacific Rise (6 °N-18 °N) (Salters et al., 2011). Reference data for intraplate basalts from the study region are the same as those in Fig. 2. (For interpretation of the references to colour in this figure legend, the reader is referred to the web version of this article.)

end-member. The increasing Ce/Pb ratio with decreasing Pb content, along with the positive Ti and Nb anomalies, in the late Cenozoic intraplate basalts from south China and south Vietnam are typical geochemical features of recycled oceanic crusts (e.g., An et al., 2017; Hoang et al., 2018; Yu et al., 2019; Zeng et al., 2017). This is because that Pb is more fluid-mobile than Ce when the oceanic crust dehydrates during subduction. Rutile is a common accessory phase in eclogite that is derived from recycled oceanic crust and Nb and Ti are highly compatible in rutile (e.g., Foley et al., 2000; Klemme et al., 2005). Thus, melts originating from recycled oceanic crusts show elevated Ce/Pb and Nb/Th ratios similar to the high-Ce/Pb component. Generally, oceanic crust consists of MORB-type pillow basalts and underlying gabbroic cumulates. The gabbroic cumulates have positive Sr and Eu anomalies reflecting plagioclase accumulation while the upper basaltic crust has no profound Sr and Eu anomalies (White and Klein, 2014). In comparison, the southeast Cambodia basalts have positive Sr anomalies and positive correlation between their ε_{Nd} and Sr/Sr* ratios ($Sr/Sr^* = 2 \times Sr_N/(Pr_N + Nd_N)$, where N indicates normalized to primitive mantle; Fig. S4a), indicating that the gabbroic cumulates of the lower oceanic crust should be a more appropriate candidate for the source of high-Ce/Pb end-member.

Nd and Hf isotopic variations have been inferred to be decoupled in global MORBs (e.g., Chauvel et al., 2008; Li et al., 2016, 2019; Pearce et al., 1999), wherein Pacific MORBs have negative $\Delta\varepsilon_{Hf}$ values and Indian MORBs have positive $\Delta\varepsilon_{Hf}$ values. Almost all oceanic sediments have elevated ε_{Hf} at a given ε_{Nd} showing positive $\Delta\varepsilon_{Hf}$ values (e.g., Chauvel et al., 2008). Therefore, the negative $\Delta\varepsilon_{Hf}$ nature of those high-Ce/Pb components from southeast Cambodia and south China points to the existence of recycled Pacific MORB-like oceanic crusts in their sources (e.g., Wang et al., 2013; Yu et al., 2019; Zeng et al., 2017) rather than recycled sediments. The high-Ce/Pb end-member in the southeast Cambodia basalts is similar to the recycled Paleo-Pacific MORB-like oceanic crust (ca. 400–500 Ma) (Fig. 4b). In comparison, the high-Ce/Pb components of the Fujian and Hainan basalts are trending to the Pacific MORB-like oceanic crusts at various ages (Fig. 4b; ca. 1.5–2.0 Ga for Fujian basalts and ca. 200–500 Ma for Hainan basalts; Wang et al., 2013; Zeng et al., 2017). In contrast, the Thailand basalts have elevated Ce/Pb and Nb/Th ratios with increasing positive $\Delta\varepsilon_{Hf}$ values (Fig. 5). This enriched component is also suggested to come from recycled oceanic crust materials (Yan et al., 2018). The positive $\Delta\varepsilon_{Hf}$ values and relative enriched Sr-Nd-Hf isotopic compositions of the Thailand basalts could be ascribed to the recycling of Indian MORB-type oceanic crust with or

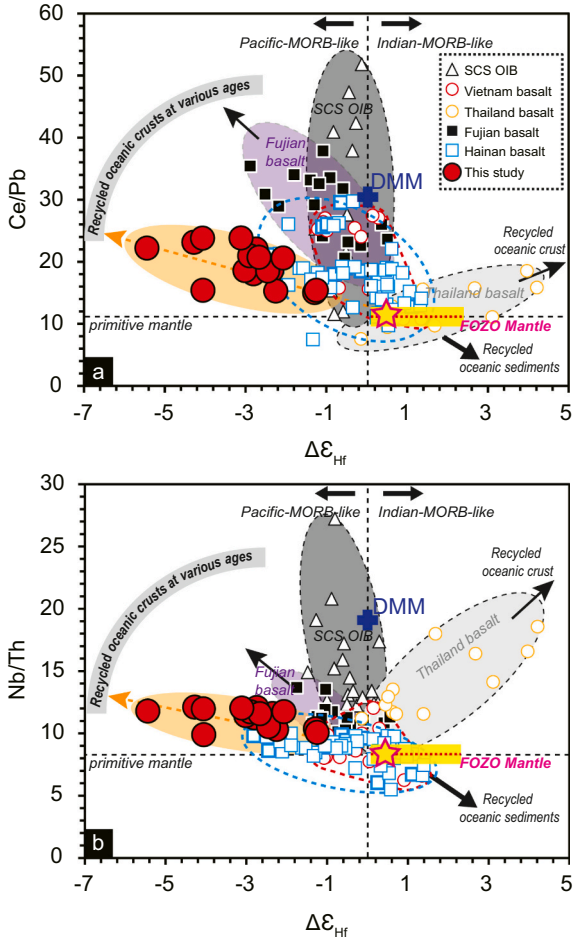

Fig. 5. Plots of Ce/Pb (a) and Nb/Th (b) versus $\Delta\varepsilon_{Hf}$ values for southeast Cambodia basalts. $\Delta\varepsilon_{Hf}$ is defined as the deviation of ε_{Hf} from the global terrestrial array, $\Delta\varepsilon_{Hf} = \varepsilon_{Hf}\text{-}1.55 \times \varepsilon_{Nd}\text{-}1.21$ (Vervoort et al., 2011). Data for depleted MORB mantle (DMM) are from Workman and Hart (2005). In both figures, the yellow star stands for the potential geochemical compositions of a common low-Ce/Pb component; the yellow belt represents the isotopic variation of the reported FOZO mantle (Jackson et al., 2007; Jackson et al., 2020; Rooney et al., 2012). Reference data for intraplate basalts from the study region are the same as those in Fig. 2. (For interpretation of the references to colour in this figure legend, the reader is referred to the web version of this article.)

without oceanic sediments in their source (Yan et al., 2018).

4.3. Characteristics of the common low-Ce/Pb component: A FOZO-like component from the deep mantle

In this study, we also identified a low Ce/Pb component with a relatively depleted isotopic composition (e.g., high ε_{Hf} values; Fig. 7a) that is present in all intraplate basalts from the South China Sea region. The mantle sources of the Hainan and southern Vietnam basalts have been reported to contain recycled pelagic sediments characterized by low Ce/Pb and Nb/Th ratios and positive $\Delta\varepsilon_{Hf}$ values (e.g., Hoang et al., 2018; Mei and Ren, 2019). However, recycled oceanic sediments in the mantle source should form basalts with enriched isotopic compositions (e.g., low ε_{Nd} and ε_{Hf} values; Fig. 4b) and elevating Th/La ratios (Fig. S4b), which are inconsistent with the geochemical characteristics of the common low-Ce/Pb component. The relatively depleted nature of this end-member might be depleted asthenospheric mantle with or without carbonated component, continental lithosphere, or potential contribution from deep lower mantle as reported (e.g., Li et al., 2020; Wang et al., 2013; Yu et al., 2019; Zou et al., 2000). In the following sections, we discuss the origin of the shared low-Ce/Pb component.

4.3.1. Depleted asthenosphere with or without a carbonated component?

Depleted MORB mantle (DMM) is a candidate for the shared isotopically depleted component (e.g., Zou et al., 2000). However, the DMM has depleted trace elemental pattern with high Ce/Pb and Nb/Th ratios which is different from the low-Ce/Pb end-member (Fig. 5). Another candidate is the carbonated component in the asthenospheric mantle with depleted Nd and Hf isotopes. Such chemical and isotopic signatures from the carbonated mantle have been widely reported for intraplate basalts in eastern China (Li et al., 2017). Cenozoic intraplate basalts derived from a carbonated source are characterized by significant negative of Zr, Hf, and Ti anomalies (i.e., low Ti/Ti* and Hf/Hf* ratios) and low SiO_2 with high CaO and CaO/Al_2O_3 ratio (Zeng et al., 2010), and results in distinctive stable Mg and Zn isotopic compositions (Li et al., 2017; Liu et al., 2016b). However, the low-Ce/Pb component exhibits decreasing CaO/Al_2O_3 ratio and Ti/Ti* ~ 1 (Fig. 7b). Therefore, depleted asthenosphere with or without carbonated component cannot be the source of the common low-Ce/Pb component.

4.3.2. Subcontinental lithospheric mantle contamination?

The subcontinental lithospheric mantle (SCLM) can modify the geochemical compositions of intraplate basalts through contamination at the asthenosphere–lithosphere boundary (e.g., Xu et al., 2005). Direct contamination forms basalts with lower abundances of highly incompatible elements, kinked rare earth element (REE) patterns, and correlations between isotopic compositions and MgO content (Xu et al., 2005). The southeast Cambodia basalts have OIB-like REE patterns (Fig. 3a) and exhibit no correlation between MgO content and ε_{Nd} value (Fig. 6b), which precludes direct lithospheric mantle contamination. Melt–rock interaction in the lithospheric mantle can also modify the geochemical compositions of basalts (Liu et al., 2016a). The La/Yb ratio can reflect the degree of melt–rock interaction, as La is more incompatible than Yb. Potassic basalts affected by melt–rock interactions exhibit a negative correlation between La/Yb ratio and MgO content, and a positive correlation between La/Yb and Rb/Nb ratios (Fig. S5a–b), due to the dissolution of olivine and precipitation of phlogopite (Liu et al., 2016a). Melt–rock interaction in the lithospheric mantle has been proposed to have affected intraplate sodic basalts from the South China Sea basin, whereby the reacted melts exhibit positive correlations between La/Yb and MgO and between La/Yb and Rb/Nb (Fig. S5a–b), due to the dissolution of orthopyroxene and precipitation of olivine and apatite (Zhang et al., 2017). In comparison, the southeast Cambodia basalts have no correlation between La/Yb and MgO, and have a negative correlation between La/Yb and Rb/Nb, which precludes potential melt–rock interactions in the lithospheric mantle. Furthermore, Sr—Nd isotopic compositions of the SCLM as represented by mantle peridotites from southeast China are more depleted than the shared low-Ce/Pb component (Fig. 4a), further excluding the role of the SCLM in modifying the compositions of the intraplate basalts.

4.3.3. Confirmation of a FOZO-like mantle component in the source of the intraplate basalts

The common low-Ce/Pb component is characterized by Ce/Pb and Nb/Th with low ratios (Fig. 5) and Ti/Ti* and Eu/Eu* with ratios ~1. It also has slightly positive $\Delta\varepsilon_{Hf}$ value, moderate $^{87}Sr/^{86}Sr$ ratio, and high ε_{Hf} value (Fig. 7c–d), similar to geochemical features of the primitive mantle (McDonough and Sun, 1995). We compared the radiogenic isotopic features of the shared low-Ce/Pb component with those of FOZO (i.e., the primitive mantle), which usually has high $^3He/^4He$ isotopic ratio that is a unique feature of the lower mantle and plume–related basalts (Jackson et al., 2007; Jackson et al., 2020; Rooney et al., 2012). In Fig. 7c–d, the common low-Ce/Pb component is located in the field close to FOZO, verifying the affinity between the low-Ce/Pb component and FOZO. The FOZO-like low-Ce/Pb component is characterized by moderate $^{87}Sr/^{86}Sr$ (~0.7040) and ε_{Nd} (~ + 5), and high ε_{Hf} (~ + 9.5).

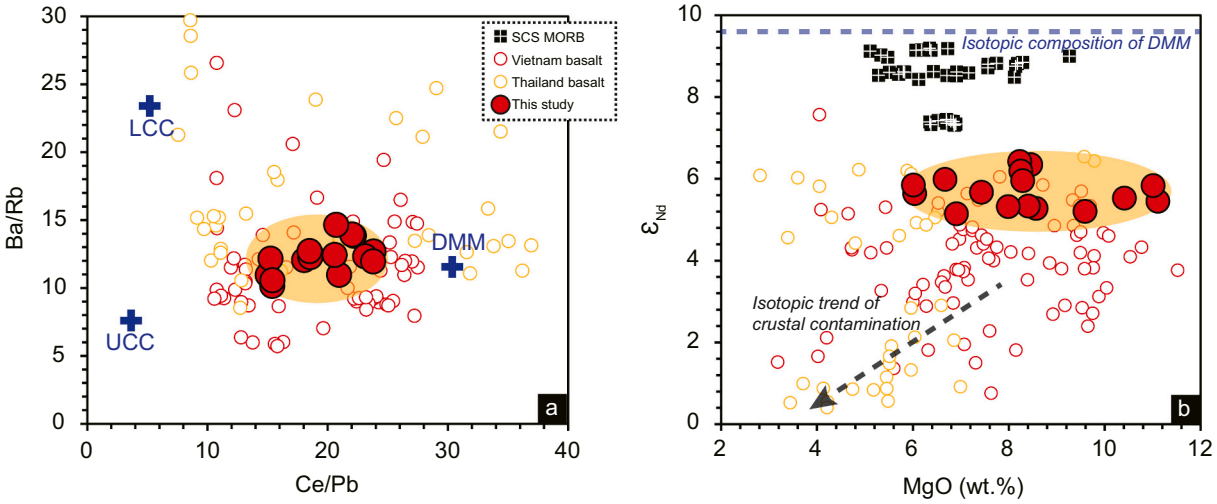

Fig. 6. Plots of Ba/Rb versus Ce/Pb (a) and ε_{Nd} versus MgO (b) for southeast Cambodia basalts. Data for the depleted MORB mantle (DMM) ($Ce/Pb_{DMM} = 30.56$, $Ba/Rb_{DMM} = 11.26$, $\varepsilon_{Nd} = +9.6$) are from Workman and Hart (2005). Data for the upper continental crust ($Ce/Pb_{UCC} = 3.71$, $Ba/Rb_{UCC} = 7.66$) and the lower continental crust ($Ce/Pb_{LCC} = 5.00$, $Ba/Rb_{LCC} = 23.55$) are from Rudnick and Gao (2014). Data of South China Sea MORB are collected from references (Zhang et al., 2018a; Zhang et al., 2018b). Reference data for intraplate basalts from Vietnam and Thailand are the same as those in Fig. 2.

Although we didn't measure the Pb isotopes of southeast Cambodia basalts, we plotted the collected data in the plot of $^{208}Pb^*/^{206}Pb^*$ versus ε_{Nd} (Fig. S6). At the same ε_{Nd} around +5, samples from south China, the South China Sea basin, and Indochina Peninsula share the same common component as we suggested. Pb and Re—Os isotopic compositions of the Hainan basalts also suggest that such a low-Ce/Pb component was derived from a FOZO-like primitive mantle source (Wang et al., 2013), which is generally inferred to be the dominant lower mantle component (Hofmann, 2014). This FOZO-like material is potentially derived from the upwelling Hainan mantle plume that has been detected by seismic observations in the case of Hainan basalts (Wang et al., 2012; Wang et al., 2013; Xu et al., 2012). In addition to the Hainan basalts, the influence of the plume has been invoked for the intraplate basalts from southern Vietnam, Thailand, the South China Sea basin, and southeast China (An et al., 2017; Hoang et al., 2018; Yan et al., 2018; Zhang et al., 2017; Zhang et al., 2018a). Recent seismic tomographic results show that, although the strongest low-Vp zones exist beneath Hainan, significant low-Vp anomalies are evident in the mantle beneath Indochina, the South China Sea, and South China. As such, a cluster of plumes has been proposed to exist, rather than a single Hainan plume (e.g., Zhao et al., 2021). Irrespective of the extent and geometry of the plume, low-Vp zones have been imaged in the lower mantle beneath the South China Sea region that extend to the upper mantle (Lei et al., 2009; Xia et al., 2016; Zhao et al., 2021). The existence of mantle plume provides the possibility for the widely distribution of FOZO-like mantle components in the study region. Our data along with previously reported geochemical and geophysical observations confirm that the common low-Ce/Pb end-member in this region is most likely derived from a deep-seated lower mantle source.

4.4. *Geodynamics of intraplate volcanism in the vicinity of a subduction system*

The origins of the low- and high-Ce/Pb components in the study region can provide insights into the deep geodynamics of the upper mantle in the vicinity of a subduction system. Since the Mesozoic, subduction of the Paleo-Pacific Plate has had an important role in controlling the tectonic evolution of southeastern Eurasia (Li and Li, 2007) and related basaltic magmatism (e.g., Zeng et al., 2016). Therefore, we suggest that the subducted Pacific MORB-type oceanic crust could be the source of the high-Ce/Pb components in the Cambodia, Fujian, and Hainan basalts. In comparison, to the nearly zero and positive $\Delta\varepsilon_{Hf}$ values of basalts from southern Vietnam and Thailand suggest that the recycled oceanic crusts in their source might be Indian MORB-like (Figs. 5, 7). Furthermore, recycled oceanic sediments existed in the mantle sources of southern Vietnam, Thailand, and Hainan basalts (e.g., Hoang et al., 2018; Mei and Ren, 2019; Yan et al., 2018) as exhibited by their low Nb/Th ratio and high Th/La ratio with positive $\Delta\varepsilon_{Hf}$ values (Figs. 5b, S4b). Therefore, in addition to the common low-Ce/Pb FOZO-like mantle component, the upper mantle beneath the South China Sea region consists of highly heterogeneous, recycled oceanic crust materials from two distinct oceanic plates.

There are two geodynamic possibilities to explain the co-existence of FOZO-like mantle and heterogeneous, recycled oceanic crusts in the same mantle source: (1) a highly heterogeneous mantle plume derived from the core–mantle boundary; (2) a mantle plume that has interacted with a reservoir containing heterogeneous, recycled oceanic crust. There is little evidence to suggest the Hainan mantle plume is highly heterogeneous (Li et al., 2020; Wang et al., 2013; Yan et al., 2018), because the Hainan basalts are isotopically relatively homogeneous (Fig. 7). Apart from the shared FOZO-like end-member, basalts from the southern Vietnam, Cambodia, Thailand, Hainan, the South China Sea basin, and Fujian exhibit different geochemical trends in Figs. 5 and 7, suggesting that the enriched components at different locations are highly heterogeneous. Such spatial variation excludes a shared highly heterogeneous mantle plume as their common enriched source. A reservoir containing highly heterogeneous, recycled oceanic materials is needed in the mixing model. Geophysical observations suggest that a stagnant cold and dense component (i.e., the Paleo-Pacific oceanic slab) is currently present in the mantle transition zone beneath southeastern China (Huang and Zhao, 2006) (Fig. 1c). Seismic tomographic observations have also identified the existence of cold and dense slabs in the mantle transition zone beneath the Indochina Block and South China Sea basin (Zhao et al., 2021) (Fig. 1c). Consequently, the subducted oceanic slabs in the mantle transition zone are likely to be an important mantle reservoir.

In addition to the large volume of stagnant oceanic crust in the mantle transition zone, large low-resistivity anomalies occur above and below the mantle transition zone beneath the South China Sea region (Huang and Zhao, 2006; Xia et al., 2016; Zhao et al., 2021) (Fig. 1c). We thus propose a geodynamic model, including the blocking of an upwelling mantle plume by the stagnant slabs, plume-slab interaction, and subsequent upwelling of secondary plumes into the upper mantle, to explain the origin of intraplate basalts in the South China Sea region (Fig. 8). The subducted oceanic slabs include both Pacific and Indian

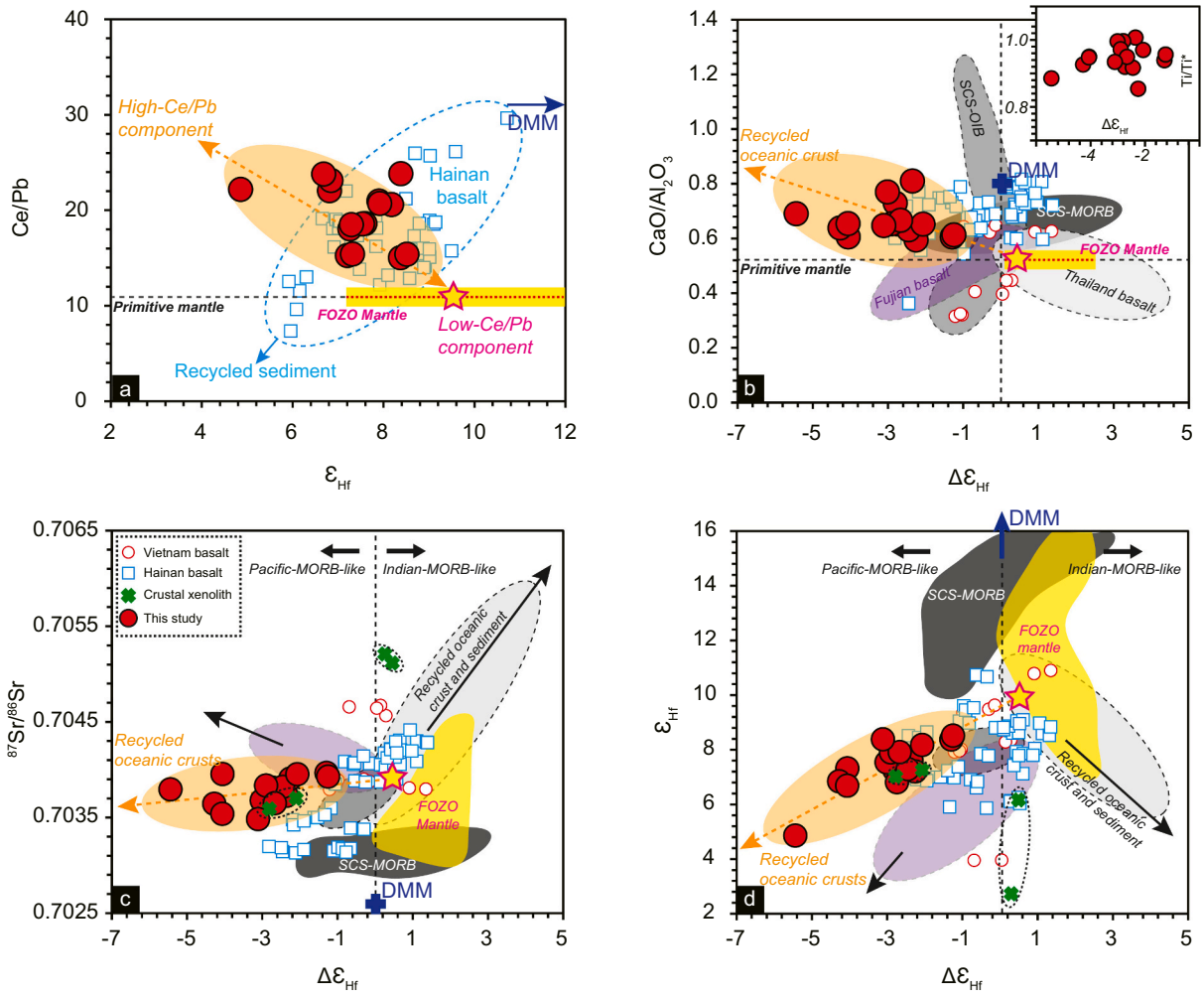

Fig. 7. Plot of Ce/Pb versus ε_{Hf} (a) and variations of CaO/Al_2O_3 (b), $^{87}Sr/^{86}Sr$ (c), and ε_{Hf} (d) versus $\Delta\varepsilon_{Hf}$ values for southeast Cambodia basalts. Data for depleted MORB mantle (DMM) are from Workman and Hart (2005). Isotopic data for FOZO mantle are collected from reference (Jackson et al., 2007; Jackson et al., 2020; Rooney et al., 2012). Data for the South China Sea MORB are from references (Zhang et al., 2018a; Zhang et al., 2018b). In all figures, the yellow star stands for the potential geochemical compositions of the common low-Ce/Pb component ($\Delta\varepsilon_{Hf} = \sim +0.5$, $^{87}Sr/^{86}Sr = \sim 0.7040$, $\varepsilon_{Hf} = \sim +9.5$); the yellow belt in figures a and b represents the isotopic compositions of the reported FOZO mantle having high $^3He/^4He$ isotopic ratios (Jackson et al., 2007; Jackson et al., 2020; Rooney et al., 2012). Reference data for intraplate basalts from study region are the same as those in Fig. 2. (For interpretation of the references to colour in this figure legend, the reader is referred to the web version of this article.)

types and they are stagnant in the mantle transition zone forming a barrier of highly heterogeneous, recycled oceanic crusts (Fig. 8). This barrier blocked the upwelling mantle plume from the core–mantle boundary prior to the mid-Miocene. Opening of the South China Sea basin strengthened convection in the upper mantle, which allowed the formation of secondary plumes from the mantle transition zone (Zhao et al., 2021). The upwelling secondary plumes contain stagnant oceanic slab material from the mantle transition zone, and underwent partial melting in the shallow mantle that formed the widely distributed post-Miocene intraplate volcanisms in the South China Sea region. One of the limitations of our model is that, while some plume-related basalts have $^3He/^4He$ values ranging from low to high, basalts from study region only have low $^3He/^4He$ ratios so far. One possibility is that the amount of data reported is still very limited. The other explanation is that the high-$^3He/^4He$ domain is denser than other components hosted in plumes (Jackson et al., 2017). Such denser materials of higher $^3He/^4He$ ratios are more difficult to be brought up by the plume that was already hindered by the stagnant slabs.

4.5. Implication

The phenomenon of reported thermal anomaly in the asthenosphere without significant signal of mantle plumes is widely seen from southeast Eurasia (e.g., An et al., 2017; Wang et al., 2012; Yang et al., 2019); however, no consistent interpretations have been obtained. Our mantle plume–stagnant slab interaction model can explain such paradox. This model also explains why the intraplate volcanism exhibits similar geochemical variations and source heterogeneity within a limited distance of the South China Sea basin. Moreover, the stagnant subducted slabs in the mantle transition zone act as a filter to modify the geochemical compositions of the upwelling plumes, further providing an interpretation for MORB-like $^3He/^4He$ ratios of some plume-related basalts. Therefore, we highlight that, in the context of a subduction system, interaction between an upwelling mantle plume and a stagnant slab in the mantle transition zone can hamper the mantle upwelling and cause isotopic heterogeneity in the upper mantle and associated basalts.

5. Conclusion

Elemental and isotopic compositions of southeast Cambodia basalts

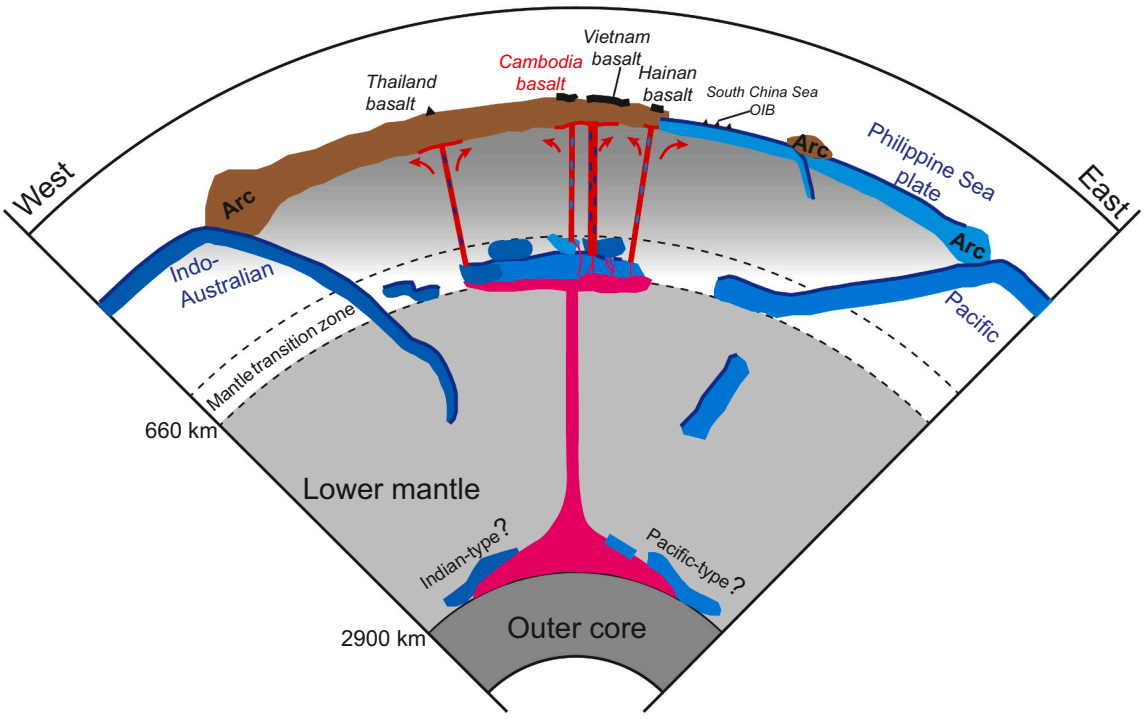

Fig. 8. Cartoon illustrating the geodynamics in forming intraplate volcanisms from southeastern Eurasia. The upwelling mantle plume from core-mantle boundary was blocked by the barriers in the mantle transition zone from the South China Sea region before the Miocene. Opening of the South China Sea strengthened the convection of the upper mantle forming secondary plumes from the mantle transition zone. Consequently, upwelling of secondary plumes formed intraplate basaltic volcanisms since the Miocene.

reveal a mixing feature of two end-member components in the mantle source of them, a FOZO-like mantle component and a Pacific MORB-like recycled oceanic crustal component. In comparison with the intraplate basalts from the Indochina Peninsula, Hainan Island, South China Sea basin, and south China, we find that the upper mantle is composed of a shared FOZO-like mantle component and recycled oceanic crusts with highly heterogeneous isotopic compositions in the South China Sea region. To interpret the regular spatial and temporal distribution of these intraplate basalts and the geochemical relationship between these basalts and mantle plume, we obtained a new petro-genesis model of mantle plume-stagnant slab interaction. Our model includes hampering of an upwelling mantle plume by the stagnant slabs, plume-slab interaction, and subsequent upwelling of secondary plumes into the upper mantle. This study provides a new dynamic model to explain the formation of continental intraplate basalts. In addition, our study provides insight into understanding the mantle plume activities in the vicinity of subduction zones. We suggest that the signal of mantle plumes can be contaminated or diluted by the stagnant subducted oceanic slabs in the mantle transition zone.

Data availability statement

The data for present study are available at figshare (https://doi.org/10.6084/m9.figshare.17170988.v1). Supplementary Materials contain details about supplementary methods, figures, and experimental data.

Declaration of Competing Interest

The authors declare that they have no known competing financial interests or personal relationships that could have appeared to influence the work reported in this paper.

Acknowledgements

This work is supported by the National Key R&D Program of China (2018YFE0202402), the National Natural Science Foundation of China (41906051), and the Shanghai Science and Technology Innovation Action Plan (20590780200). We thank Wen-Li Xie and Liang Li for their technical help during lab work and Jingwen Zhang for collecting part of data. Dr. Yanwei Zhang, Mr. Wei Shu, Mr. Lork Hong, and Mr. Soeun DoE Va attended the field investigations of the Cambodia basalts.

Appendix A. Supplementary data

Supplementary data to this article can be found online at https://doi.org/10.1016/j.lithos.2022.106795.

References

An, A.R., Choi, S.H., Yu, Y., Lee, D.C., 2017. Petrogenesis of late Cenozoic basaltic rocks from southern Vietnam. Lithos 272-273, 192–204.
Anders, E., Grevesse, N., 1989. Abundances of the elements: Meteoritic and solar. Geochim. Cosmochim. Acta 53, 197–214.
Barr, S.M., Macdonald, A.S., 1981. Geochemistry and geochronology of late Cenozoic basalts of Southeast Asia: Summary. Geol. Soc. Am. Bull. 92, 508–512.
Carlson, R.W., Lugmair, G.W., Macdougall, J.D., 1981. Columbia River volcanism: the question of mantle heterogeneity or crustal contamination. Geochim. Cosmochim. Acta 45 (12), 2483–2499.
Chang, S.J., Ferreira, A.M., Faccenda, M., 2016. Upper- and mid-mantle interaction between the Samoan plume and the Tonga-Kermadec slabs. Nat. Commun. 7, 10799.
Chauvel, C., Lewin, E., Carpentier, M., Arndt, N.T., Marini, J.C., 2008. Role of recycled oceanic basalt and sediment in generating the Hf-Nd mantle-array. Nat. Geosci. 1 (1), 64–67.
Chen, L.H., Zeng, G., Jiang, S.Y., Hofmann, A.W., Xu, X.S., Pan, M.B., 2009. Sources of Anfengshan basalts: Subducted lower crust in the Sulu UHP belt, China. Earth Planet. Sci. Lett. 286, 426–435.
Christiansen, R.L., Foulger, G.R., Evans, J.R., 2002. Upper mantle origin of the Yellowstone hot spot. Geol. Soc. Am. Bull. 114, 1245–1256.
Condie, K.C., 2001. Mantle Plumes and their Record in Earth History. Cambridge University Press, Cambridge.
Fletcher, M., Wyman, D.A., 2015. Mantle plume-subduction zone interactions over the past 60 Ma. Lithos 233, 162–173.

Flower, M.F.J., Zhang, M., Chen, C.-Y., Tu, K., Xie, G., 1992. Magmatism in the South China Basin: 2. Post-spreading Quaternary basalts from Hainan Island, South China. Chem. Geol. 97, 65–87.
Foley, S.F., Barth, M.G., Jenner, G.A., 2000. Rutile/melt partition coefficients for trace elements and an assessment of the influence of rutile on the trace element characteristics of subduction zone magmas. Geochim. Cosmochim. Acta 64, 933–938.
Hall, R., 2002. Cenozoic geological and plate tectonic evolution of SE Asia and the SW Pacific: Computer-based reconstructions, model and animations. J. Asian Earth Sci. 20, 353–431.
Ho, K.-S., Chen, J.-C., Lo, C.-H., Zhao, H.-L., 2003. ^{40}Ar–^{39}Ar dating and geochemical characteristics of late Cenozoic basaltic rocks from the Zhejiang–Fujian region, SE China: Eruption ages, magma evolution and petrogenesis. Chem. Geol. 197, 287–318.
Hoang, N., Flower, M., 1998. Petrogenesis of Cenozoic basalts from Vietnam: Implication for origins of a 'Diffuse Igneous Province'. J. Petrol. 39, 369–395.
Hoang, N., Flower, M.F.J., Carlson, R.W., 1996. Major, trace element, and isotopic compositions of Vietnamese basalts: Interaction of hydrous EM1-rich asthenosphere with thinned Eurasian lithosphere. Geochim. Cosmochim. Acta 60, 4329–4351.
Hoàng, N., Flower, M.F.J., Chí, C.T., Xuân, P.T., Quý, H.V., Sơn, T.T., 2013. Collision-induced basalt eruptions at Pleiku and Buôn Mê Thuột, south-Central Viet Nam. J. Geodyn. 69, 65–83.
Hoang, T.H.A., Choi, S.H., Yu, Y., Pham, T.H., Nguyen, K.H., Ryu, J.-S., 2018. Geochemical constraints on the spatial distribution of recycled oceanic crust in the mantle source of late Cenozoic basalts, Vietnam. Lithos 296-299, 382–395.
Hofmann, A.W., 2014. Sampling mantle heterogeneity through oceanic basalts: Isotopes and trace elements. In: Holland, H.D., Turekian, K.K. (Eds.), Treatise on Geochemistry, Second edition. Elsevier, Oxford.
Huang, J., Zhao, D., 2006. High-resolution mantle tomography of China and surrounding regions. J. Geophys. Res-Sol. Ea. 111 (B9), 4813–4825.
Jackson, M., Kurz, M., Hart, S., Workman, R., 2007. New Samoan lavas from Ofu Island reveal a hemispherically heterogeneous high $^{3}He/^{4}He$ mantle. Earth Planet. Sci. Lett. 264, 360–374.
Jackson, M.G., Konter, J.G., Becker, T.W., 2017. Primordial helium entrained by the hottest mantle plumes. Nature 542, 340–346.
Jackson, M.G., Blichert-Toft, J., Halldorsson, S.A., Mundl-Petermeier, A., Bizimis, M., Kurz, M.D., Price, A.A., Haroardottir, S., Willhite, L.N., Breddam, K., Becker, T.W., Fischer, R.A., 2020. Ancient helium and tungsten isotopic signatures preserved in mantle domains least modified by crustal recycling. Proc. Natl. Acad. Sci. U. S. A. 117 (49), 30993–31001.
Kincaid, C., Ito, G., Gable, C., 1995. Laboratory investigation of the interaction of off-axis mantle plumes and spreading centers. Nature 376, 758–761.
Kincaid, C., Druken, K.A., Griffiths, R.W., Stegman, D.R., 2013. Bifurcation of the Yellowstone plume driven by subduction induced mantle flow. Nat. Geosci. 6, 395–399.
Klemme, S., Prowatke, S., Hametner, K., Gunther, D., 2005. Partitioning of trace elements between rutile and silicate melts: Implications for subduction zones. Geochim. Cosmochim. Acta 69, 2361–2371.
Kumar, K.V., Chavan, C., Sawant, S., Raju, K.N., Kanakdande, P., Patode, S., Deshpande, K., Krishnamacharyulu, S., Vaideswaran, T., Balaram, V., 2010. Geochemical investigation of a semi-continuous extrusive basaltic section from the Deccan Volcanic Province, India: Implications for the mantle and magma chamber processes. Contrib. Mineral. Petrol. 159 (6), 839–862.
Le Bas, M.J., Le Maitre, R.W., Streckeisen, A., Zanettin, B., 1986. A chemical classification of volcanic rocks based on the total alkali-silica diagram. J. Petrol. 27, 745–750.
Lei, J., Zhao, D., Steinberger, B., Wu, B., Shen, F., Li, Z., 2009. New seismic constraints on the upper mantle structure of the Hainan plume. Phys. Earth Planet. Inter. 173, 33–50.
Leonard, T., Liu, L., 2016. The role of a mantle plume in the formation of Yellowstone volcanism. Geophys. Res. Lett. 43, 1132–1139.
Li, Z.X., Li, X.H., 2007. Formation of the 1300-km-wide intracontinental orogen and postorogenic magmatic province in Mesozoic South China: a flat-slab subduction model. Geology 35, 179–182.
Li, C.F., Lin, J., Kulhanek, D.K., Williams, T., Bao, R., Briais, A., Brown, E.A., Chen, Y., Clift, P.D., Colwell, F.S., Dadd, K.A., Ding, W., Hernandez-Almeida, I., Huang, X., Hyun, S., Jiang, T., Koppers, A.A.P., Li, Q., Liu, C., Liu, Q., Liu, Z., Nagai, R.H., Peleo-Alampay, A., Su, X., Sun, Z., Tejada, M.L., Trinh, S.H., Yeh, Y.-C., Zhang, C., Zhang, F., Zhang, G.-L., Zhao, X., Tang, H., 2014. Opening of the South China Sea and its implications for southeast Asian tectonics, climates, and deep mantle processes since the late Mesozoic. Int. Ocean Disc. Progr. Prelim. Rep. 349 https://doi.org/10.14379/iodp.pr.349.2014, 1-109.
Li, H.-Y., Xu, Y.-G., Ryan, J.G., Huang, X.-L., Ren, Z.-Y., Guo, H., Ning, Z.-G., 2016. Olivine and melt inclusion chemical constraints on the source of intracontinental basalts from the eastern North China Craton: Discrimination of contributions from the subducted Pacific slab. Geochim. Cosmochim. Acta 178, 1–19.
Li, S.-G., Yang, W., Ke, S., Meng, X., Tian, H., Xu, L., He, Y., Huang, J., Wang, X.-C., Xia, Q., 2017. Deep carbon cycles constrained by a large-scale mantle Mg isotope anomaly in eastern China. Natl. Sci. Rev. 4, 111–120.
Li, H.-Y., Taylor, R.N., Prytulak, J., Kirchenbaur, M., Shervais, J.W., Ryan, J.G., Godard, M., Reagan, M.K., Pearce, J.A., 2019. Radiogenic isotopes document the start of subduction in the Western Pacific. Earth Planet. Sci. Lett. 518, 197–210.
Li, Y.-Q., Kitagawa, H., Nakamura, E., Ma, C., Hu, X., Kobayashi, K., Sakaguchi, C., 2020. Various ages of recycled material in the source of Cenozoic basalts in SE China: Implications for the role of the Hainan plume. J. Petrol. 61 (6) doi: 10/1093/petrology/egaa060.
Liu, J.-Q., Chen, L.-H., Zeng, G., Wang, X.-J., Zhong, Y., Yu, X., 2016a. Lithospheric thickness controlled compositional variations in potassic basalts of Northeast China by melt-rock interactions. Geophys. Res. Lett. 43, 2582–2589.
Liu, S.A., Wang, Z.Z., Li, S.G., Huang, J., Yang, W., 2016b. Zinc isotope evidence for a large-scale carbonated mantle beneath eastern China. Earth Planet. Sci. Lett. 444, 169–178.
McDonough, W.F., Sun, S.S., 1995. The composition of the Earth. Chem. Geol. 120, 223–253.
Mei, S., Ren, Z., 2019. Features and age of recycled material in mantle source of Cenozoic basaltic lavas in Hainan Island: evidence from Hf-Sr-Nd-Pb isotopic compositions. Geotecton. Metallog. 43, 1036–1051.
Mériaux, C.A., Duarte, J.C., Schellart, W.P., Mériaux, A.-S., 2015. A two-way interaction between the Hainan plume and the Manila subduction zone. Geophys. Res. Lett. 42, 5796–5802.
Mériaux, C.A., Mériaux, A.S., Schellart, W.P., Duarte, J.C., Duarte, S.S., Chen, Z., 2016. Mantle plumes in the vicinity of subduction zones. Earth Planet. Sci. Lett. 454, 166–177.
Niu, Y., O'Hara, M.J., 2003. Origin of ocean island basalts: a new perspective from petrology, geochemistry and mineral physics considerations. J. Geophys. Res-Sol. Ea. 108 (2209) https://doi.org/10.1029/2002JB002048.
Pearce, J.A., Kempton, P.D., Nowell, G.M., Noble, S.R., 1999. Hf–Nd element and isotope perspective on the nature and provenance of mantle and subduction components in western Pacific arc-basin systems. J. Petrol. 40, 1579–1611.
Pearce, J.A., Kempton, P.D., Gill, J.B., 2007. Hf–Nd evidence for the origin and distribution of mantle domains in the SW Pacific. Earth Planet. Sci. Lett. 260, 98–114.
Qi, Q., Taylor, L.A., Zhou, X., 1995. Petrology and geochemistry of mantle peridotite xenoliths from SE China. J. Petrol. 36 (1), 55–79.
Qian, S., Gazel, E., Nichols, A.R.L., Cheng, H., Zhang, L., Salters, V.J., Li, J., Xia, X., Zhou, H., 2021. The origin of late Cenozoic magmatism in the South China Sea and Southeast Asia. Geochem. Geophys. Geosyst. 22 (8) https://doi.org/10.1029/2021GC009686.
Rooney, T.O., Hanan, B.B., Graham, D.W., Furman, T., Blichert-Toft, J., Schilling, J.-G., 2012. Upper mantle pollution during Afar plume–continental rift interaction. J. Petrol. 53, 365–389.
Rudnick, R.L., Gao, S., 2014. Composition of the continental crust. In: Holland, H.D., Turekian, K.K. (Eds.), Treatise on Geochemistry, Second edition. Elsevier, Oxford.
Salters, V.J.M., Mallick, S., Hart, S.R., Langmuir, C.E., Stracker, A., 2011. Domains of depleted mantle: New evidence from hafnium and neodymium isotopes. Geochem. Geophys. Geosyst. 12 https://doi.org/10.1029/2011GC003617.
Sun, W., 2016. Initiation and evolution of the South China Sea: An overview. Acta Geochim. 35, 215–225.
Tatsumoto, M., Basu, A.R., Huang, W., Wang, J., Xie, G., 1992. Sr, Nd, and Pb isotopes of ultramafic xenoliths in volcanic rocks of Eastern China: Enriched components EMI and EMII in subcontinental lithosphere. Earth Planet. Sci. Lett. 113 (1–2), 107–128.
Tu, K., Flower, M.F.J., Carlson, R.W., Zhang, M., Xie, G., 1991. Sr, Nd, and Pb isotopic compositions of Hainan basalts (South China): Implications for a subcontinental lithosphere Dupal source. Geology 19, 567–569.
Tu, K., Flower, M.F.J., Carlson, R.W., Xie, G., Chen, C.-Y., Zhang, M., 1992. Magmatism in the South China Basin: 1. Isotopic and trace-element evidence for an endogenous Dupal mantle component. Chem. Geol. 97, 47–63.
Vervoort, J.D., Plank, T., Prytulak, J., 2011. The Hf–Nd isotopic composition of marine sediments. Geochim. Cosmochim. Acta 75, 5903–5926.
Wang, X.-C., Li, Z.-X., Li, X.-H., Li, J., Liu, Y., Long, W.-G., Zhou, J.-B., Wang, F., 2012. Temperature, pressure, and composition of the mantle source region of late Cenozoic basalts in Hainan Island, SE Asia: a consequence of a young thermal mantle plume close to subduction zones? J. Petrol. 53, 177–233.
Wang, X.-C., Li, Z.-X., Li, X.-H., Li, J., Xu, Y.-G., Li, X.-H., 2013. Identification of an ancient mantle reservoir and young recycled materials in the source region of a young mantle plume: Implications for potential linkages between plume and plate tectonics. Earth Planet. Sci. Lett. 377–378, 248–259.
White, W.M., Klein, E.M., 2014. Composition of the oceanic crust. In: Holland, H.D., Turekian, K.K. (Eds.), Treatise on Geochemistry, Second edition. Elsevier, Oxford.
White, W.M., Mcbirney, A.R., Duncan, R.A., 1993. Petrology and geochemistry of the Galápagos Islands: portrait of a pathological mantle plume. J. Geophys. Res-Sol. Ea. 98 https://doi.org/10.1029/1093JB02018.
Workman, R.K., Hart, S.R., 2005. Major and trace element composition of the depleted MORB mantle (DMM). Earth Planet. Sci. Lett. 231, 53–72.
Xia, S., Zhao, D., Sun, J., Huang, H., 2016. Teleseismic imaging of the mantle beneath southernmost China: New insights into the Hainan plume. Gondwana Res. 36, 46–56.
Xu, Y.-G., Ma, J.-L., Frey, F.A., Feigenson, M.D., Liu, J.-F., 2005. Role of lithosphere–asthenosphere interaction in the genesis of Quaternary alkali and tholeiitic basalts from Datong, western North China Craton. Chem. Geol. 224, 247–271.
Xu, Y.G., Wei, J.X., Qiu, H.N., Zhang, H.H., Huang, X.L., 2012. Opening and evolution of the South China Sea constrained by studies on volcanic rocks: preliminary results and a research design. Chin. Sci. Bull. 57, 1863–1878.
Yan, Q.S., Shi, X.F., 2008. Olivine chemistry of Cenozoic basalts in the South China Sea and the potential temperature of the mantle. Acta Petrol. Sin. 24, 176–184.
Yan, Q., Shi, X., Wang, K., Bu, W., Xiao, L., 2008. Major element, trace element, and Sr, Nd and Pb isotope studies of Cenozoic basalts from the South China Sea. Sci. China Ser. D 51, 550–566.
Yan, Q., Castillo, P., Shi, X., Wang, L., Liao, L., Ren, J., 2015. Geochemistry and petrogenesis of volcanic rocks from Daimao Seamount (South China Sea) and their tectonic implications. Lithos 218–219, 117–126.

Yan, Q., Shi, X., Metcalfe, I., Liu, S., Xu, T., Kornkanitnan, N., Sirichaiseth, T., Yuan, L., Zhang, Y., Zhang, H., 2018. Hainan mantle plume produced late Cenozoic basaltic rocks in Thailand, Southeast Asia. Sci. Rep. 8 (1), 2640. https://doi.org/10.1038/s41598-018-20712-7.

Yang, F., Huang, X.-L., Xu, Y.-G., He, P.-L., 2019. Plume-ridge interaction in the South China Sea: Thermometric evidence from Hole U1431E of IODP Expedition 349. Lithos 324-325, 466–478.

Yasuda, A., Fujii, T., 1998. Ascending subducted oceanic crust entrained within mantle plumes. Geophys. Res. Lett. 25, 1561–1564.

Yu, J.-H., Xu, X.-S., O'Reilly, S.Y., Griffin, W.L., Zhang, M., 2003. Granulite xenoliths from Cenozoic Basalts in SE China provide geochemical fingerprints to distinguish lower crust terranes from the North and South China tectonic blocks. Lithos 67, 77–102.

Yu, X., Lee, C.T.A., Chen, L.H., Zeng, G., 2015. Magmatic recharge in continental flood basalts: Insights from the Chifeng igneous province in Inner Mongolia. Geochem. Geophys. Geosyst. 16 (7), 2082–2096.

Yu, X., Zeng, G., Chen, L.-H., Wang, X.-J., Liu, J.-Q., Xie, L.-W., Yang, T., 2019. Evidence for rutile-bearing eclogite in the mantle sources of the Cenozoic Zhejiang basalts, eastern China. Lithos 324-325, 152–164.

Zeng, G., Chen, L.-H., Hofmann, A.W., Jiang, S.-Y., Xu, X.-S., 2011. Crust recycling in the sources of two parallel volcanic chains in Shandong, North China. Earth Planet. Sci. Lett. 302, 359–368.

Zeng, G., Chen, L.-H., Xu, X.-S., Jiang, S.-Y., Hofmann, A.W., 2010. Carbonated mantle sources for Cenozoic intra-plate alkaline basalts in Shandong, North China. Chem. Geol. 273, 35–45.

Zeng, G., He, Z.-Y., Li, Z., Xu, X.-S., Chen, L.-H., 2016. Geodynamics of paleo-Pacific plate subduction constrained by the source lithologies of Late Mesozoic basalts in southeastern China. Geophys. Res. Lett. 43, 10189–10197.

Zeng, G., Chen, L.H., Yu, X., Liu, J.Q., Xu, X.S., Erdmann, S., 2017. Magma-magma interaction in the mantle beneath eastern China. J. Geophys. Res-Sol. Ea. 122, 2763–2769.

Zhang, G.L., Chen, L.H., Jackson, M.G., Hofmann, A.W., 2017. Evolution of carbonated melt to alkali basalt in the South China Sea. Nat. Geosci. 10, 229–235.

Zhang, G.-L., Sun, W.-D., Seward, G., 2018a. Mantle source and magmatic evolution of the dying spreading ridge in the South China Sea. Geochem. Geophys. Geosyst. 19, 4385–4399.

Zhang, G.L., Luo, Q., Zhao, J., Jackson, M.G., Guo, L.S., Zhong, L.F., 2018b. Geochemical nature of sub-ridge mantle and opening dynamics of the South China Sea. Earth Planet. Sci. Lett. 489, 145–155.

Zhao, D., Toyokuni, G., Kurata, K., 2021. Deep mantle structure and origin of Cenozoic intraplate volcanoes in Indochina, Hainan and South China Sea. Geophys. J. Int. 225, 572–588.

Zhou, P., Mukasa, S.B., 1997. Nd-Sr-Pb isotopic, and major- and trace-element geochemistry of Cenozoic lavas from the Khorat Plateau, Thailand: sources and petrogenesis. Chem. Geol. 137, 175–193.

Zou, H., Zindler, A., Xu, X., Qi, Q., 2000. Major, trace element, and Nd, Sr and Pb isotope studies of Cenozoic basalts in SE China: Mantle sources, regional variations, and tectonic significance. Chem. Geol. 171, 33–47.